polymer papers

Transmission electron microscopic investigation of the morphology of a poly(hydroxybenzoate-*co*-hydroxynaphthoate) liquid crystal polymer

Steven D. Hudson* and Andrew J. Lovinger
AT&T Bell Laboratories, Murray Hill, NJ 07974, USA
(Received 15 June 1992)

The semicrystalline morphology of a 73:27 mol% poly(hydroxybenzoate-*co*-hydroxynaphthoate) liquid crystal polymer is studied via transmission electron microscopy (TEM) and wide-angle X-ray diffraction. A permanganic etchant was used for TEM sample preparation and the etchant composition was optimized for selectivity of the non-crystalline phase. Crystalline lamellae, developed during cooling from the nematic phase, measure approximately 10 nm in thickness and 100 nm laterally. The lamellae are periodic, having a repeat of 34 nm. Because the molecules are long (~200 nm) and extended, tie chains between lamellae are abundant. Crystallization must therefore occur via small axial shifts of approximately a monomer length. Based on our observations of disclination morphologies, the splay elastic constant is greater than that for bend, indicating considerable molecular semiflexibility. The interior morphology of bulk injection-moulded specimens is also revealed following microtomy and selective etching. Molecular orientation and defect density can be accurately measured.

(Keywords: liquid crystal polymers; morphology; electron microscopy)

INTRODUCTION

Liquid crystal polymers (LCPs) are a major class of polymeric materials of commercial importance because of their high-temperature and high-strength properties, their dimensional stabilities and low coefficients of thermal expansion. Their local molecular alignment, inherent in the nematic liquid-crystalline phase, facilitates the production of highly aligned and thus very strong and rigid fibres and tapes[1]. More recently these materials have also been attracting increasing interest for injection moulding applications[2], because their low melt viscosity is desirable for processing. The commercially available LCPs are also notable for their rapid crystallization, which permits extremely rapid moulding cycle times. In addition, their lack of densification upon solidification facilitates high-precision moulding, which is becoming increasingly important.

The most common commercial thermotropic LCP is a random copolyester of hydroxybenzoic and hydroxynaphthoic acids (HBA and HNA, respectively). Its random comonomeric sequence, verified by X-ray scattering[3], destabilizes the crystalline phase, thus promoting the liquid crystalline phase. Nevertheless, crystallization is still possible and may be detected either by thermal analysis or by X-ray diffraction[4]. The exact structure of the crystalline phase has not been determined, but it is clear that the crystals are composed of random chains. The aperiodic spacing of the diffraction spots is predicted by the convolution of the two monomeric units[5]. Two general models of crystallization have been proposed and have been the subject of considerable debate[6,7]; these models are discussed further in this paper.

Crystallization upon cooling is very rapid; in fact it has not been possible to quench the nematic to the glassy state without some crystallization[8]. Typically, the per cent crystallinity of quenched samples, as measured by X-ray diffraction[8], is approximately 30%. The crystallinity and crystal perfection may be increased with annealing[4], allowing crystallinities to reach ~60%. Annealing, especially at temperatures near the melting transition, also affects the chain packing. At low crystallization temperatures, the lateral packing is hexagonal, while at higher crystallization temperatures it is orthorhombic[9]. The orthorhombic form has a higher melting temperature, which for 73/27 mol% HBA/HNA is approximately 320°C. The morphology has been revealed by dark-field electron microscopy[7,10]. Crystallites are lamellar in shape, approximately 15 nm thick (along the chain) and 100 nm long (in the lateral direction). The lamellae also have somewhat irregular boundaries.

In this paper, we present morphological investigations using a permanganic etchant that preferentially removes more disordered material, revealing the semicrystalline morphology. Olley and Bassett have successfully used such elective etchants to investigate the morphology of bulk samples of other melt-crystallized polymers[11]. Recently, Hanna *et al.* have applied similar etchants to these liquid crystalline random copolymers[12]. We have optimized the etchant composition to reveal clearly the periodic lamellar morphology. In addition, observation of this morphology enables high resolution information

* To whom correspondence should be addressed

0032-3861/93/061123-07

regarding the local molecular orientation. Larger-scale morphology, i.e. variation and quality of the molecular alignment, has been investigated in LCPs by a number of authors using various techniques. The morphology was revealed at a gross level by fracturing the sample, since fracture parallel to the polymer chain direction is easier than perpendicular to it[13]. Average properties of the molecular orientation were also probed via thermal conductivity[14] or birefringence[15] measurements. The technique employed here differs from the above in that it offers nearly molecular resolution of the variations of the molecular orientation throughout a sample of interest.

METHOD

Vectra A950 was obtained from Hoechst-Celanese in the form of pellets. This polymer has a comonomer ratio of 73/27 (HBA/HNA)[16]. The melting temperature of this composition is 280°C, and its glass transition is at approximately 130°C[9]. This melt temperature is therefore sufficiently low that the material can be melt-processed without chemical degradation. Films of Vectra A950 were prepared by melt shearing of solid pellets onto a heated glass coverslip held at approximately 320°C. After equilibrating for approximately 30 s at that temperature, the material was quenched to ambient by quickly removing the coverslip from the hotplate. Bulk-moulded samples were also investigated. These samples were in the shape of a standard tensile specimen 160 mm in length with a cross section of 3×12 mm. They had been injection-moulded with the gate at one end of the mould, so that the flow direction was along the length, the primary gradient direction was along the thickness, and the neutral direction was along the width of the samples. The temperature of the LCP melt during moulding was 300°C, while the mould was held at 95°C. It was filled in approximately 1 s (giving a shear rate in the mould cavity of approximately $50\,s^{-1}$), and the cycle time was 30 s. Some samples were annealed in air at approximately 210°C for 2 h.

The crystallinity of the samples was determined using a Rigaku X-ray diffractometer at room temperature. The orientation and texture of the thinner sections of the films were observed via polarizing optical microscopy. A Reichert-Jung sliding microtome was used to cut sequentially $\sim 50\ \mu m$ thick sections of the moulded tensile samples. The surface of a microtomed section or an external surface of either a moulded or a thin-film sample could then be etched.

The etchant we employed was similar to that developed by Olley and Bassett[11]. Finely ground potassium permanganate was dissolved in a mixture of H_2O, H_3PO_4 and H_2SO_4. The temperature of the etchant was approximately 30°C. After many trials, we concluded that the optimal etchant composition was 0.5 wt% $KMnO_4$ with a solvent ratio of 2:2:1 (H_2O:H_3PO_4:H_2SO_4). This etchant selectively removes the more disordered material in a clean fashion and without introducing artifacts, and thus leaves the surface protruding with lamellar crystals. The lamellae can then be imaged by a replication process.

The replication employed was in one or two steps. To prepare a two-stage replica, a concentrated aqueous solution of poly(acrylic acid) (PAA) was cast onto the polymer. After the water evaporated, the glassy PAA was detached from the surface, shadowed with platinum and coated with carbon. The final Pt/C replica was obtained by dissolving the PAA in water. To prepare a one-stage (or direct) replica, the LCP itself was directly shadowed with platinum and coated with carbon. The direct replica could be either detached with PAA or separated by dissolving the LCP in fuming sulfuric acid. In this latter case, the PAA (if used) plays only a passive role as a temporary backing. The two methods of replication give different information, primarily because the LCP adheres to either the PAA (in the two-step process) or the Pt/C (in the one-step process), and a thin layer of polymer fibrils may thus be detached from the surface. The *fracture* surface is shadowed in the two-step process, whereas the *etched* surface of the detached polymer layer is shadowed in the one-step process. These effects are described in the following section. Finally, the replicas were examined in bright field in a Jeol 100CX transmission electron microscope at 100 kV.

RESULTS AND DISCUSSION

The crystallinity of the various samples was first explored using wide-angle X-ray diffraction. The most intense scattering is associated with lateral correlations between chains. In the nematic state, liquid-like intermolecular ordering produces a broad and diffuse peak at approximately 0.49 nm[4]. The room-temperature diffractogram of a quenched thin film (*Figure 1a*) contains sharper peaks, which are associated with crystallinity. Crystallinities were measured by subtracting the contribution from the disordered peak as defined in reference 4. The major peak is the 1 1 0 reflection at 0.45 nm, while the less-resolved peak at 0.33 nm corresponds to the 2 1 1 and 2 1 0 reflections[9]. Annealing at 209°C for 2 h has little effect on the structure (*Figure 1b*). The crystals become slightly more perfect (reflected in the small decrease in the breadth of the 1 1 0 peak), but the overall crystallinity remains at about 28%. Longer annealing at perhaps higher

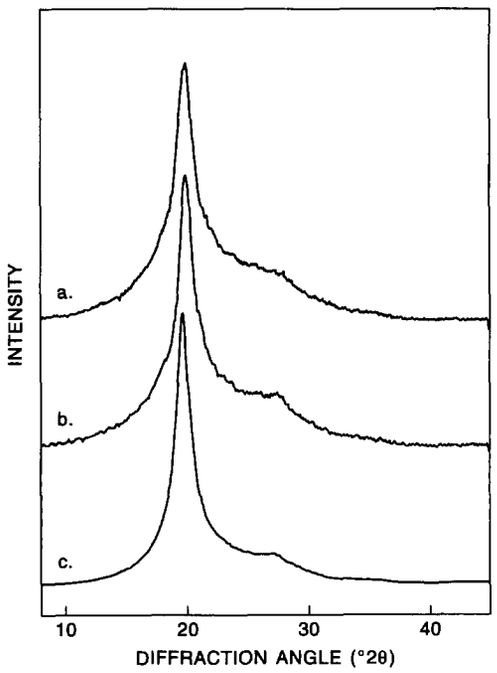

Figure 1 Wide angle X-ray diffractograms for (a) a quenched thin film, (b) the film in (a) annealed at 210°C for 2 h, and (c) an injection-moulded bulk specimen

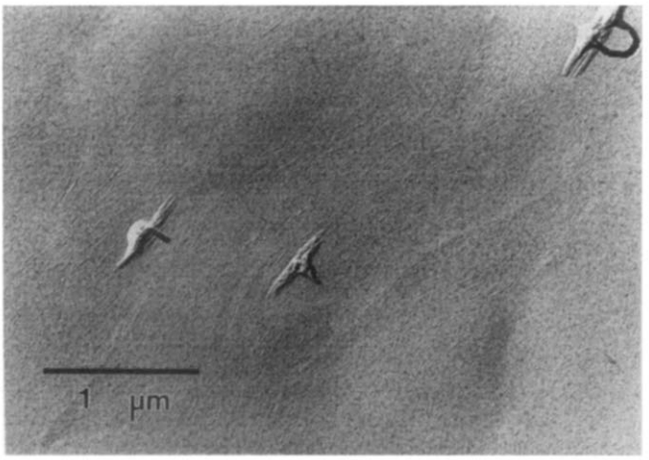

Figure 2 TEM micrograph of a two-stage replica of an unetched film. Variously sized fibrils of LCP adhered to the poly(acrylic acid) during detachment. The molecular axis is parallel to the fibrils

temperatures would be required to increase crystallinity significantly[8]. Moulded samples, which are cooled less rapidly because of their greater thickness, possess higher crystallinities. Typical values are ~44% (*Figure 1c*), and the intermolecular diffuse peak is reduced in comparison to those of *Figures 1a* and *b*. To learn further details of the semicrystalline morphology, electron microscopy was employed.

The first effect examined by transmission electron microscopy (TEM) is detachment of unetched polymer by the PAA replica (*Figure 2*). This is useful as a control in understanding the effects of the etchant. A variety of fibrillar morphologies can be observed in this micrograph. Three large fibril groupings approximately 0.5 μm long and 50–100 nm in width constitute the most prominent features. The dark serpentine ribbons extending from these three are fibrils that were pulled away from the replica surface. In addition to these three large fibril groupings, the surface is covered by finer fibrils (~200 × 20 nm). Even though the sample is 28% crystalline, there is no morphological evidence of lamellar crystals in this figure. The invisibility of the lamellae is principally a result of the lack of chain folding. The persistence length in a good solvent was measured to be 12 nm (approximately 16 monomer units)[17], making these polymer chains sufficiently stiff to prevent tight folding. In the liquid-crystalline phase, the nematic field is probably sufficient to extend the molecules. Because the molecules are extended in both the liquid crystalline and the crystalline phase, the mechanical properties of the lamellae and the interlamellar regions are similar, so that fibrillation is not very sensitive to the semicrystalline morphology. Furthermore, because the density difference between crystal and frozen nematic is negligible, crystallites are not observable within the fibres in bright-field TEM.

This method of preparation also reveals (albeit somewhat crudely) the molecular orientation, which appears sinuous but generally along the shear direction (from lower left to upper right of the figure). The shadowing also shows that the surface has weak undulations, with the crests approximately parallel to the shear. Although the local molecular orientation can be discerned, the resolution is poor because the detachment of polymer is not uniform throughout an area. The contrast is likewise very poor because the fibrils are typically very thin.

Much more information may be obtained if the polymer is first etched and then replicated via the two-step process (*Figure 3*). Once again, a variety of fibrillar morphologies are observed, ranging from large fibril groupings to very thin fibrils. The surface of the polymer appears to have been weakened by the etchant so that a greater number of larger polymeric fibrils were detached. In this figure, the shear direction is nearly horizontal, and the largest fibrils are removed from along the crests of the film undulations. The Pt shadowing direction is from the lower right in *Figure 3*, and the thick fibrils cast long shadows (which appear as bright images in this figure). In the shadows of these thick fibrils, polymer lamellae can be clearly discerned. The contrast in these light regions arises presumably from the difference in thickness within the detached film. The more slowly-etched lamellae have a greater thickness and thus appear darker. The morphology of these lamellae is in general agreement with previous dark-field observations[6]. The crystallite dimension is approximately 10 nm along the chain direction and approximately 100 nm long laterally. The lamellae also appear to be irregularly shaped.

Most of the detached polymer fibrils are too thin to be imaged by thickness contrast and are therefore invisible in the bright regions. Outside of these lighter regions, however, the fracture surface of the detached polymer layer was exposed to the Pt shadowing. In these regions, lamellae are apparent, but fibrils are now clearly revealed. The surface that is being shadowed has little if any lamellar detail; similar to that shown in *Figure 2*. As expected, the fibrils are indeed seen to be orthogonal to the lamellae. As a further indication that the lamellae are visualized via thickness contrast produced by differential etch rates, the lamellae do not generally cast a shadow in the regions exposed by the Pt. To get an idea of the magnitude of the differential etch rates, we note that larger, thicker fibrils (which are approximately 10 nm thick) can be observed in the bright regions by thickness contrast.

If we wish to discern preferentially the *lamellae* rather than the *fibrils*, a direct-replication process must be used (see *Figure 4*). The most striking and informative characteristic of these lamellae is that they have a regular and uniform period. In this image, this

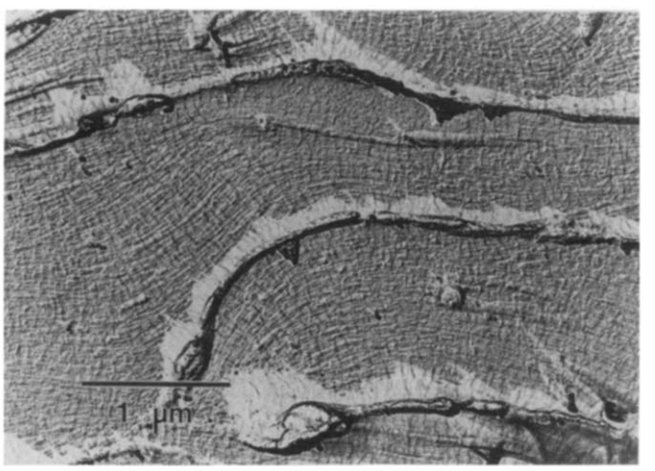

Figure 3 TEM micrograph of a two-stage replica of a film etched in 1 wt% $KMnO_4$ solution in 2:2:1 H_2O:H_3PO_4:H_2SO_4 for 3 h at 30°C. Both lamellae and fibrils are revealed

period is approximately 37 nm. We have not observed this period to vary significantly in any of our specimens, which, however, had all been crystallized at large undercoolings. The average period measured from all our specimens is approximately 34 nm, the lateral size of the lamellae is approximately 100 nm, and the height of the protruding lamellae, estimated from shadow lengths, is approximately 10 nm.

The image differs not only because the external surface is shadowed directly, but also because the adhesion of the polymer to the Pt/C differs from that to the PAA. The detached fibrils are now thicker and more sparse. They are, in fact, sufficiently thick to allow recording of electron diffraction patterns (inset in *Figure 4*), which confirm that the molecular axis is along the polymer fibril and perpendicular to the lamellae. Using the equatorial reflection as an internal calibration at 0.45 nm, the meridional reflections are observed at 0.671 and 0.209 nm. Values of 0.670 and 0.209 nm have been reported previously[3] for a copolymer having a comonomer ratio of 75/25, and are associated with the convolution of two monomeric repeat units.

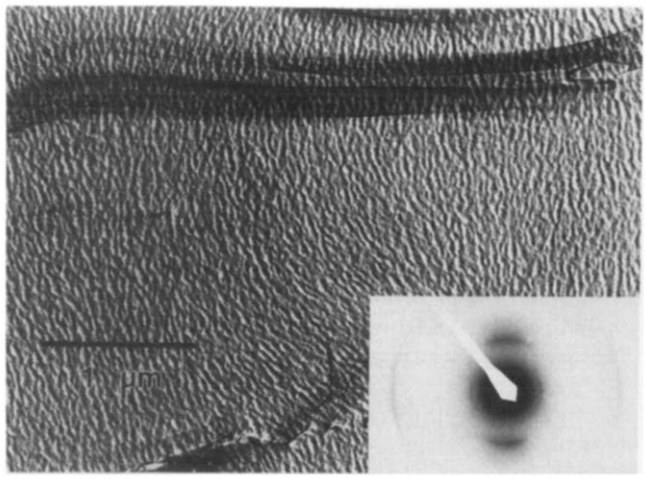

Figure 4 TEM micrograph of a direct replica detached from a film etched in 0.5 wt% $KMnO_4$ solution in 2:2:1 H_2O:H_3PO_4:H_2SO_4 for 1 h at 30°C. Inset is a diffraction pattern from the detached polymer fibril at the top of the micrograph

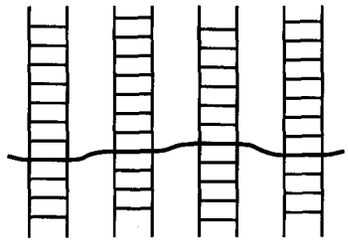

Figure 5 Schematic showing an extended semiflexible chain incorporated into a periodic lamellar morphology

For further insight into the crystal morphology of this relatively rigid random copolymer, knowledge of the molecular weight is important. Using a suitable solvent (3,5-bis(trifluoromethyl)phenol), light scattering and g.p.c. results gave M_n and M_w as 13.8 and 43.9 kg mol^{-1}, respectively[17] (measurements from the supplier[18] yielded similar results: 14.7 and 38.2 kg mol^{-1}, respectively). The weight-average molecular length is therefore approximately 200 nm, which is six times the lamellar repeat. Because tight folds are impossible, the morphological picture which emerges is that of lamellar crystals bridged by many tie chains, and of the average chain having segments incorporated in several different lamellar crystals (as shown schematically in *Figure 5*). This picture has profound consequences on the mechanism of crystallization.

Crystals, in general, must possess some degree of three-dimensional order (both lateral and axial). However, in this case, a relatively rigid chain (where the persistence length is nearly equal to the interlamellar distance)[17] must optimize its axial position in one crystal, even though it is tied to crystals on either side. Therefore, limited axial shifts, at most a few monomer lengths, are expected, imposing restrictions to the degree of order attained.

As mentioned in the Introduction, two general categories of crystallization model have been proposed. We now discuss the implications of our morphology for these models. The earliest model was put forth by Windle *et al.*[6] and is illustrated in *Figure 6a*. In this proposal, aperiodic three-dimensional crystalline order

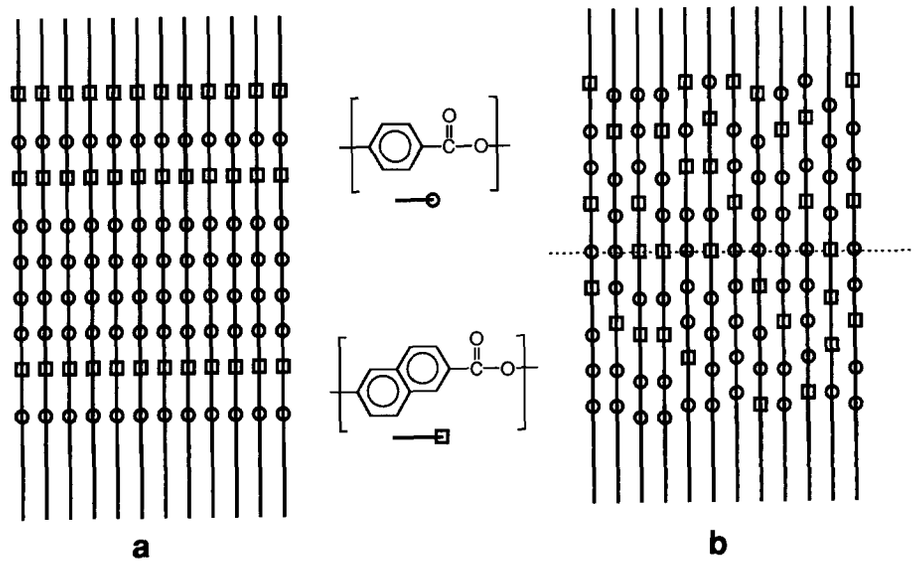

Figure 6 Schematic representation of two proposed crystallization models for lamellae in rigid random copolymers: (a) reference 6 and (b) reference 7

is established through aggregation of identical random sequences. This idea has been used to justify sharply diffracting entities (crystalline lamellae) observed in dark-field TEM. Biswas and Blackwell[7] subsequently proposed a different model where three-dimensional crystalline order is established through packing and axial registry of (non-identical) random chains (*Figure 6b*). This model is supported mostly by diffraction data. The chemical similarity of the two monomers contributes to increased order. Both monomers are aromatic and have ester linkages; they differ only in size. Significant long-range, albeit frustrated, crystalline order is possible. This ordering is facilitated by the monomer lengths (0.635 nm: 0.837 nm), which have a nearly low-integer rational relation ($\sim$3:4). Most recently, Hanna *et al.*[12] have proposed a modification that incorporates the basic features of both models: a short segment of matched sequences[6] provides a sort of nucleus for the type of crystal described in reference 7.

These models each have consequences for the morphology. In the first model, as originally developed in reference 6, the crystal thickness along the chain is limited by the probability of aggregating identical sequences of random chain. In the second[7], however, the thickness is not inherently limited and might be expected to depend upon crystallization conditions. The two models also predict different lamellar periods. In the first model, matching of monomer sequences of consistent length with the lamellar thickness requires 'searching' nearly the full length of neighbouring chains. The axial shifts between chains during crystallization are therefore on the order of a large fraction of the molecular length. This also implies that the lamellar separation will be on the order of the molecular length. Fortuitous secondary sequence matching cannot produce crystals of any considerable extent[19]. The crystallinity therefore decreases with increasing chain length. To obtain crystallinities of 30%, Hanna and Windle[19] predict chains having a degree of polymerization less than 20. This model is therefore inconsistent with our observed morphology, in which we demonstrate uniform lamellar repeats that are much smaller than the molecular length.

In the second model, however, the lamellar period is not constrained by the length of the molecular chains. Because the shifts required for axial registry are not of the order of the molecular length, but are instead less than a *monomer* unit length, small axial shifts are sufficient. Therefore, the morphological evidence that we present lends further support for the basic model of reference 7. However, we cannot exclude some small degree of matching of very short sequences at the core of these lamellae, so that discrimination between the model of reference 7 and its recently proposed modification[12] is not possible.

The chain-sequence-matching model of reference 6 would be aided if transesterification (which involves rearrangement of the chemical sequence of a chain) could occur rapidly on the time scale of crystallization; as we have discussed, the latter should be on the order of seconds at 200°C. Through transesterification, monomers could rearrange during crystallization in order to build up identical sequences. However, the reaction rate is too slow. Using neutron diffraction, MacDonald *et al.*[20] have studied the transesterification of a rigid-chain polymer similar to HBA/HNA, revealing that these rearrangements require days at 200°C.

To return to morphological features uncovered by our etching method, a lower-magnification image of a direct replica detached from the surface is shown in *Figure 7a*. Once again, several fibrils, which appear dark in the image, are observed to be perpendicular to the lamellar orientation. The long bright features which are loosely perpendicular to the lamellae are tears in the replica. Moreover, disclinations are revealed. The disclinations in this figure are all of half-integer strength, meaning that the director rotates by π radians in the neighbourhood of the defect. Previous observations of disclinations in thin films of semiflexible LCPs allow measurement of the anisotropy of splay and bend elastic constants[21]. Although we have not made precise measurements for this random copolymer, a qualitative estimate of the elastic anisotropy can be made from visual inspection. Because the lamellae are orthogonal to the molecular director, bend of lamellae implies molecular splay and vice versa. Since there is an excess of molecular bend distortion in the neighbourhood of the positive disclinations (the lamellae in these regions splay considerably, regardless of disclination orientation), the splay constant for this polymer is expected to be large compared to the bend constant. The difference in elastic

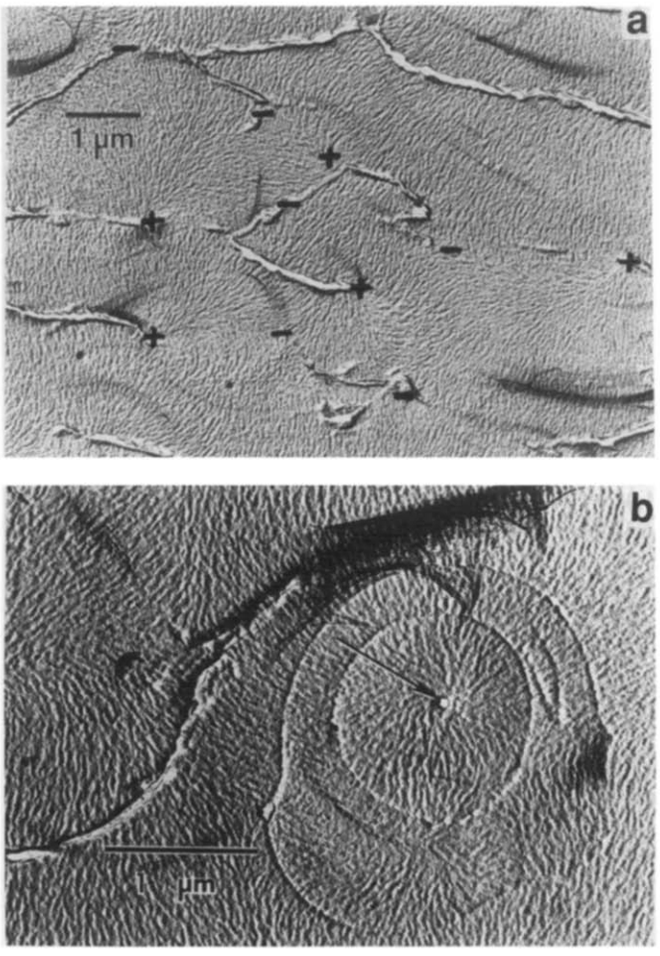

Figure 7 (a) Lower magnification TEM image of the replica in *Figure 4*. Half-integer disclinations are marked with + and − signs. Note that the lamellae are less visible when parallel to the shadowing direction (nearly horizontal). (b) TEM micrograph of a direct replica detached from a film etched in 0.2 wt% $KMnO_4$ solution in 2:2:1 H_2O:H_3PO_4:H_2SO_4 for 2 h at 30°C. An integer disclination is shown by an arrow. The molecules bend in a circular fashion about the defect. The disclination core appears unescaped, because the director field is two-dimensional in a thin film

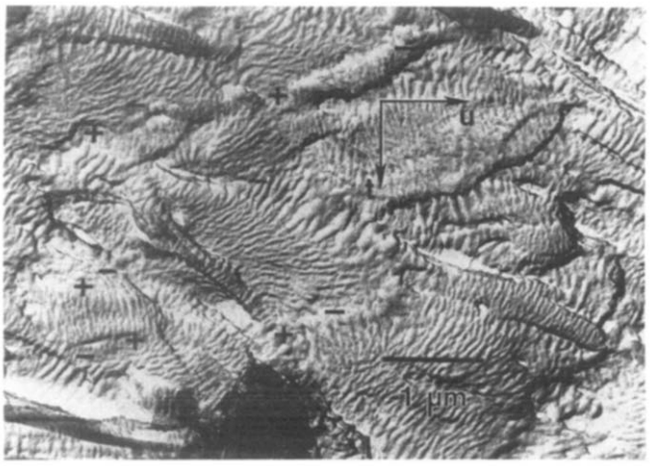

Figure 8 Replica of an internal surface of a bulk sample. The flow, **u**, and the thickness, **t**, directions are identified. In some regions, the period of the lamellae appears to increase, indicating tilt of the molecular director away from the surface plane. In the central region, the period is approximately three times the inherent period, indicating a 70° tilt out of the plane of the surface

constants is confirmed by the structure of positive integer disclinations (*Figure 7b*). In this case, the lamellae radiate from the defect, indicating tangentially oriented molecules bending around the defect. This is the stable structure if the splay constant is greater than the bend constant.

The elastic constants are indicative of molecular structure. Splay, which requires aggregation of chain ends, is costly, because the molecules are long ($L_w \approx 200$ nm) and not folded. Bend, on the other hand, is independent of molecular weight, depending only on the persistence length. (In solution the persistence length was found to be 12 nm or 1/16 of the molecular length[17].) The morphological features at low magnification (disclinations) therefore reveal a similar molecular structure to that discussed above: the molecules are fully extended, yet flexible and worm-like.

The ability to image directly the lamellae inherent in the LCP offers a distinct advantage, at least in principle, over an external decoration, such as with evaporated polyethylene. This is because the LCP lamellae have a characteristic period, so that the *three-dimensional* orientation of the director can be revealed. As we have already mentioned, the period of the lamellae in our various planar thin-film samples is approximately 34 nm per repeat. If the molecular orientation is inclined with respect to the surface, the *apparent* period of the lamellae will be increased. We have observed this in bulk samples where the molecules are not restricted to lie parallel to the arbitrary internal surface produced by microtomy. *Figure 8* shows a replica from the interior of an injection-moulded tensile specimen, where the section surface is parallel to both the shear and gradient directions and is taken approximately 70 mm from the gate. The material at this point has experienced more than 20 shear units since entering the mould cavity, so that the morphology should have reached steady state. Typical sections reveal that the molecular director lies preferentially in the shear and neutral directions of the specimen (i.e. along its length and width, respectively). Therefore, images of sections parallel to the gradient (i.e. thickness) direction are dominated by out-of-plane distortion, and images of those sections normal to the gradient direction should have nearly uniform apparent lamellar periodicity and be dominated by azimuthal variations.

We present this figure, however, to demonstrate how azimuthal and out-of-plane distortions may be observed *simultaneously*. In the centre of the figure, the out-of-plane orientation is greatest and is at least 70°. In other regions, the apparent lamellar period approaches the inherent period and the molecules are nearly parallel to the surface of the section. Throughout most of the figure, the out-of-plane orientation is intermediate. Disclinations are apparent as long as there is azimuthal variation; they have been highlighted in the figure. Based on a number of images, the disclination density in the interior of the sample is 10^7–10^8 cm^{-2}. Disclinations become very hard to observe when the director variation is exclusively out-of-plane. In this case, in order to detect disclinations, it is necessary to be able to distinguish the lamellae tilting towards the shadowing direction from those that are tilting away. This has not been possible, since it requires detection of small differences in shadow length and intensity projected on an uneven substrate. Therefore only the magnitude and not the direction of tilt is detectable.

Having described the semicrystalline lamellar morphology as revealed by permanganic etching, the effects of etchant composition are now discussed. The action of the etchant is determined most sensitively by the ratio of water to acid mixture used to dissolve the potassium permanganate. Up to this point, our results were for two parts water and three parts acid (which itself was a mixture of phosphoric and sulfuric acids in a ratio of 2:1). On the other hand, if no water is used to dilute the etchant, the etching rate is much more rapid and the attack appears preferential in a different manner. *Figure 9* shows this through a direct replica of the surface of a thin film that has been etched in 1 wt% $KMnO_4$ in 0:2:1 H_2O:H_3PO_4:H_2SO_4 solution for 15 min at 30°C. This particular composition leaves the surface much rougher. Regions of uniform molecular orientation appear much more mottled and various striations are present. The most apparent striation is that along the molecular axis. Lamellae are also revealed, as highlighted by the arrow in the upper right portion of the figure. In that region of the figure, the molecular orientation is parallel to the arrow, and the arrowed lamella is perpendicular to it. A

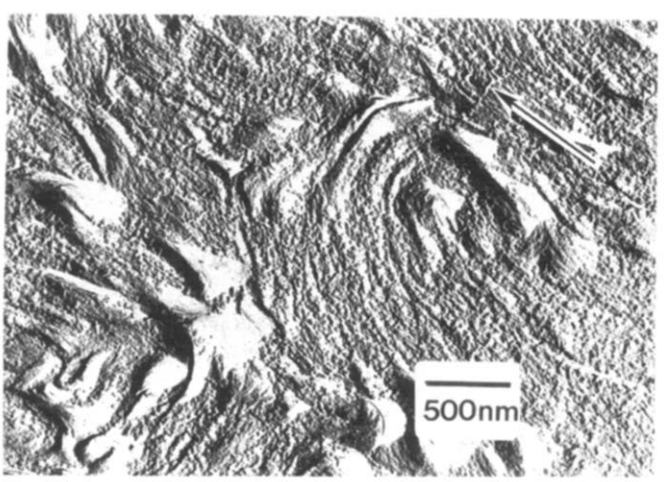

Figure 9 Direct replica of a film as etched in 1 wt% $KMnO_4$ solution in 0:2:1 H_2O:H_3PO_4:H_2SO_4 for 15 min at 30°C. Both the chain axis and the lamellae are revealed

unique characteristic of this composition is that it not only reveals the lamellae, but also highlights the molecular orientation. Note that striations parallel to the molecules are inherent in the etched surface and are not polymer fibrils. To prove this, the replica shown in *Figure 9* was not detached from the polymer. Instead the polymer was dissolved away using fuming sulfuric acid. In addition to the roughness and striations at a fine scale, the etch rate is highly non-uniform over larger distances; it is especially slow in the neighbourhood of the disclination defects.

The etching also depends on the ratio of phosphoric and sulfuric acids in the acid mixture. Their proportion was varied while keeping the ratio of water to acid mixture at 2:3, i.e. so that lamellae are revealed. If phosphoric and sulfuric acids are used in a 1:1 ratio, no striations are observed and the etched surface is quite smooth. If the ratio is 9:1 or 1:0, lamellae are only weakly observed. Therefore the ratio of 2:1 is nearly optimal for revealing lamellae. Finally, the etching behaviour is insensitive to $KMnO_4$ concentration from 1 to 0.1 wt% (as demonstrated in *Figures 3*, *4* and *7*).

CONCLUSIONS

We have optimized the use of a potassium permanganic etchant, similar to that developed by Olley and Bassett[11], for use in elucidating the semicrystalline morphology of HBA/HNA random LCPs. We show that the action of the etchant is sensitive to its composition, in particular to the acidity of the solvent. With proper conditions, crystalline lamellae may be observed. The non-crystalline frozen nematic material is selectively etched, leaving the small (10×100 nm), irregularly shaped lamellar crystallites protruding from the surface. The lamellae, which form rapidly upon cooling from the mesophase, are periodically spaced at approximately 34 nm, i.e. about one-sixth of the molecular length (~ 200 nm).

We also present evidence that the splay elastic constant is greater than the bend elastic constant, indicating, in accord with previous light-scattering data from dilute solution, that the molecules are flexible, yet long and extended. In the semicrystalline state, therefore, lamellae are linked by profuse tie chains. Thus when a replica is detached, the polymer easily fibrillates. The per cent crystallinity has been measured by wide-angle X-ray scattering to be 28–44% in various samples. This morphology requires that only slight axial shifts occur for lamellar crystallization, lending further support for the model of reference 7.

The periodic nature of the lamellae has also been exploited to reveal the local molecular orientation. The molecular director is normal to the lamellae; thus azimuthal orientation of the director is revealed by that of the lamellae, and out-of-plane director orientation is elucidated by an apparent increase in the lamellar period. Based upon observations of bulk samples, this combined lamellar decoration and etching technique holds promise for revealing technologically important morphological features in bulk injection-moulded parts and correlating them with processing in order to improve the properties of these important liquid-crystalline polymeric materials.

ACKNOWLEDGEMENT

The authors are grateful for provision of injection-moulded samples by Sundar Venkataraman.

REFERENCES

1 Calundann, G. W. and Jaffe, M. *Proc. Robert A. Welch Conf. Chem. Res.* 1982, **26**, 247
2 Gabriele, M. C. *Plast. Tech.* 1990, **36** (4), 92
3 Blackwell, J., Gutierrez, G. A. and Chivers, R. A. *Macromolecules* 1984, **17**, 1219
4 Butzbach, G. D., Wendorff, J. H. and Zimmerman, H. J. *Makromol. Chem., Rapid Commun.* 1985, **6**, 821
5 Biswas, A. and Blackwell, J. *Macromolecules* 1988, **21**, 3146
6 Windle, A. H., Viney, C., Gulombok, R., Donald, A. M. and Mitchell, G. R. *Faraday Disc. Chem. Soc.* 1985, **79**, 55
7 Biswas, A. and Blackwell, J. *Macromolecules* 1988, **21**, 3152
8 Butzbach, G. D., Wendorff, J. H. and Zimmerman, H. J. *Polymer* 1986, **27**, 1337
9 Kaito, A., Kyotani, M. and Nakayama, K. *Macromolecules* 1990, **23**, 1035
10 Spontak, R. J. and Windle, A. H. *J. Polym. Sci., Polym. Phys. Edn* 1992, **30**, 61
11 Olley, R. H. and Bassett, D. C. *Polymer* 1982, **23**, 1707
12 Hanna, S., Lemmon, T. J., Spontak, R. J. and Windle, A. H. *Polymer* 1992, **33**, 3
13 Sawyer, L. C. and Jaffe, M. *J. Mater. Sci.* 1986, **21**, 1897
14 Choy, C. L., Leung, W. P. and Kwok, K. W. *Polym. Commun.* 1991, **32**, 285
15 Horio, M., Kamei, E. and Yao, S. *Nihon Reorji Gakkaishi, Soc. Rheol., Japan* 1991, **19**, 4
16 Lin, Y. G. and Winter, H. H. *Macromolecules* 1988, **21**, 2439
17 Kromer, H., Kuhn, R., Pielartzik, H., Siebke, W., Eckhardt, V. and Schmidt, M. *Macromolecules* 1991, **24**, 1950
18 Lawler, J. Hoechst-Celanese, personal communication, 1992
19 Hanna, S. and Windle, A. H. *Polymer* 1988, **29**, 207
20 MacDonald, W. A., McLenaghan, A. D. W., McLean, G., Richards, R. W. and King, S. M. *Macromolecules* 1991, **24**, 6164
21 Hudson, S. D. and Thomas, E. L. *Phys. Rev. Lett.* 1989, **62**, 1993